J.J. Ipus et al. Intermetallics 84 (2017) 30-34. http://dx.doi.org/10.1016/j.intermet.2016.12.022

Grinding and particle size selection as a procedure to enhance the magnetocaloric response of $La(Fe,Si)_{13}$ bulk samples

J. J. Ipus, J. M. Borrego, L. M. Moreno-Ramírez, J. S. Blázquez*, V. Franco, A. Conde

Dpto. Física de la Materia Condensada, Instituto de Ciencia de Materiales, C.S.I.C., Universidad de Sevilla, P.O. Box 1065, 41080 Sevilla, Spain.

* corresponding author email: jsebas@us.es

Abstract

The magnetocaloric effect of $La(Fe,Si)_{13}$ samples deteriorates with the presence of secondary phases. However, it is highly challenging to produce single phase samples by conventional procedures and purification requires long annealing time. We propose grinding and particle size selection of non-optimal starting samples as procedure to enhance the magnetocaloric response. In this study a starting multiphase $LaFe_{11.8}Si_{1.2}$ ingot was grinded and sieved to select three different particle size ranges. X-ray diffraction and Mössbauer spectrometry reveal that all samples mainly contain fcc-$La(Fe,Si)_{13}$ and bcc-Fe(Si) phases. Microstructural and magnetic results show that the fcc-$La(Fe,Si)_{13}$ phase fraction increases for samples with the smallest average particle size, increasing their magnetocaloric response in a factor larger than three with respect to that of the bulk sample.

Keywords: Magnetocaloric effect, $La(Fe,Si)_{13}$, Mössbauer spectrometry

Introduction

The magnetocaloric effect (MCE) and the search for magnetic materials with large MCE close to room temperature (RT) have received extensive attention from the research community due to the prominent application of RT magnetic refrigeration [1,2,3]. This environmental friendly technology, more energetically efficient, is called to substitute the current gas compression refrigerators.

Traditionally, pure gadolinium has been the paradigmatic material for magnetic refrigeration around RT and commonly used as a working material into devices. However, this material presents some disadvantages such as its scarcity and its high cost, which limit the use of Gd for commercial applications.

Nowadays, the research of magnetocaloric materials for RT applications is focused in giant magnetocaloric compounds as $Gd_5(Si,Ge)_4$, MnFeP(Si,Ge), NiMn-based Heusler alloys and $La(Fe,Si)_{13}$ type alloys [4,5,6,7] which, in general, suffer a field induced coupled magnetostructural transition, responsible for the large MCE. Among them, $La(Fe,Si)_{13}$ compounds are interesting materials as they have a small amount of rare earth element (La) and a high amount of Fe leading to a material with large magnetic moment and large magnetocaloric response. Moreover, they also present the possibility to tune the Curie temperature by tailoring the Si content in the alloy [8] or by adding a small amount of another element, e.g. Co or H [9,10,11]. Concerning the Si content of the alloy, x, it is observed that the fcc-$LaFe_{13-x}Si_x$ phase ($NaZn_{13}$-type structure) presents a first order phase transition in the range of $1.0 \leq x \leq 1.6$ [12]. On the other hand, if the Si content is in the range of $1.6 < x \leq 2.0$, this fcc phase presents a second order magnetic transition leading to a broader but smaller entropy change peak [13]. If the Si content is even larger, the formation of the tetragonal LaFeSi phase occurs [14].

The procedure followed to obtain an almost pure $La(Fe,Si)_{13}$ material is not easy and long-time annealing at high temperature is generally required. Even in these cases, residual phases as ferromagnetic bcc-Fe(Si) and paramagnetic tetragonal LaFeSi are generally obtained. In some circumstances, the resulting sample is not optimal. The aim of this work is to propose a procedure to increase the amount of $La(Fe,Si)_{13}$ phase without remelting the sample. Results show that it is possible to increase the fraction of the fcc-$La(Fe,Si)_{13}$ and consequently the MCE response with respect to the initial bulk sample by grinding and particle size selection.

Previous studies on particle size effects on MCE of powders samples can be found in the literature but the target studied differs from ours. Hu et al. [15], studying single phase samples, found a slight decrease of MCE as particle size reduces by grinding $(La,Ce)(Fe,Si)_{13}C_{0.2}$ alloy. In our case, the MCE enhancement is due to a reduction of the secondary phase fraction by selecting particle sizes, which does not apply to Hu et al. study. Liu et al. [16] studied the relationship between particle size and MCE in ball milled powders. In this case, the authors explain the deterioration of the MCE as milling progresses and particle size reduces due to the microstructural evolution in the samples caused by the high energy involved in the grinding process. The manual grinding performed in our study does not produce significant microstructural changes but just the fracture of the bulk sample in powder particles which sizes depend on their brittleness. Mechanical milling would imply much larger energies with the possibility of microstructural changes not desired in this work.

Experimental

Ingots of alloy with nominal composition $LaFe_{11.8}Si_{1.2}$ were prepared via arc melting under argon atmosphere. The ingot was melted several times in order to enhance the homogeneity of the material. After that, pieces of the material were sealed in a quartz crucible under vacuum, annealed at 1373 K for 7 days and then quenched in iced water in order to retain the metastable fcc-$La(Fe,Si)_{13}$ phase at RT. After the annealing treatment the pieces were hand grinded using an agate mortar. The resulting powder was sieved obtaining samples with different particle size ranges: powder particles larger than 300 μm (D_{300} sample), powder particles in the range of 100-300 μm (D_{100} sample) and powder particles in the range of 25-100 μm (D_{25} sample).

The microstructure was studied by X-ray diffraction using Cu-Kα radiation in a Bruker D8I diffractometer and Rietveld refinement of the diffraction patterns was performed using the TOPAS software. The local environment of Fe atoms was analyzed by Mössbauer spectrometry at RT in a transmission geometry using a $^{57}Co(Rh)$ source. Hyperfine parameters were obtained by fitting with NORMOS software [17] and the isomer shift (*IS*) was quoted relative to that of an α-Fe foil at RT. Scanning electron microscopy (SEM) and energy dispersive spectroscopy (EDX) of the powder samples

were performed using a Jeol JSM-6460 LV, equipped with an Incax-sight analyzer of Oxford Instruments.

Magnetic properties were studied using a Lakeshore 7407 vibrating sample magnetometer. Isothermal magnetization curves were measured from 100 to 320 K up to a maximum applied magnetic field of 1.5 T. The powder samples were pressed in silver capsules in order to prevent powder movement during measurements and to minimize the demagnetizing factor. A hydrostatic press (2 tons) was used to obtain discs of 5 mm diameter and ~0.3 mm thick. In this type of samples, the demagnetizing factor, N_d, can be obtained as [18]:

$$N_d = N_{part} + f\left(N_{pack} - N_{part}\right) \quad (1)$$

where N_{part} and N_{pack} are the demagnetizing factors of the particles and the package, respectively, and f the packing fraction. Assuming spherical particles, $N_{part} \sim 1/3$, disc shaped package with negligible height and field applied in plane, $N_{pack} \sim 0$, and $f \sim 0.5$, a value of $N_d = 0.16$ is obtained, in agreement with the magnetization behavior at low fields (the inverse of the susceptibility at $\mu_0 H<0.05$ T is approximately 0.2). In order to take into account the demagnetizing field, internal field, H, was calculated as: $H = H_{app} - N_d M$, where H_{app} is the applied field and M is the magnetization.

Isothermal magnetic entropy change, ΔS_M, was calculated from magnetization curves using Maxwell relation as:

$$\Delta S_M = \mu_0 \int_0^H \left(\frac{\partial M}{\partial T}\right)_H dH \quad (2)$$

where T is the temperature and H the maximum magnetic field. This procedure was performed with the help of the Magnetocaloric Effect Analysis Program [19].

Results and Discussion

XRD patterns of the sieved samples are shown in figure 1. From Rietveld refinement (also shown in figure 1) two phases are detected: a fcc-La(Fe,Si)$_{13}$ phase with a NaZn$_{13}$ type structure and a bcc-Fe(Si) one, with average lattice parameters a= 11.479 (2) Å and a=

2.863 (1) Å, respectively. Some of the diffraction peaks with very low intensity could be assigned to traces of tetragonal LaFeSi phase. Figure 2 shows the fraction of fcc-$La(Fe,Si)_{13}$ phase, considering only the two indexed phases, as a function of the powder particle size. As observed, it increases as the average particle size decreases. The lattice parameter of the bcc-Fe(Si) phase is consistent with a composition $Fe_{91}Si_9$ [20]. This ratio between Fe and Si content in the bcc phase is similar to the Fe/Si ratio of the $LaFe_{11.8}Si_{1.2}$ composition and, thus, the ratio in the fcc phase should also keep the nominal value. The lattice parameter measured in this study for the fcc-$La(Fe,Si)_{13}$ phase is in agreement with the data reported by Niitsu et al. [21] taking into account the nominal composition.

Backscattered electron (BSE) images of samples D_{25} and D_{300} (figure 3) reveal the presence of three different zones. The dark and grey zones could be related to the previously referred bcc-Fe(Si) and fcc-$La(Fe,Si)_{13}$ phases, respectively. In addition, minority brighter spots are present and could be ascribed to the tetragonal LaFeSi phase with a larger molar mass (74.28 g/mol) than those of fcc-$LaFe_{11.8}Si_{1.2}$ (59.40 g/mol) and bcc-$Fe_{91}Si_9$ (53.35 g/mol). EDX confirms the enrichment in La content as the brightness of the region increases.

In order to extract some quantitative information, a similar rectangular area of exploration was selected in both images. For D_{300} sample a fraction of about 14 % of the area corresponds to the bcc-Fe(Si) type phase, while for D_{25} only about 6 % of the area is covered by dark regions. Only ~1 % of the area corresponds to the tetragonal LaFeSi phase for both samples. This result agrees with a non-clear detection of this phase by X-ray diffraction. The dependence of the fraction of each phase on the powder particle size could be ascribed to the influence in the grinding of the different mechanical properties. In fact, the intermetallic fcc-$La(Fe,Si)_{13}$ is a brittle material whereas the bcc-Fe(Si) phase is a ductile one [9].

Mössbauer spectroscopy allowed us to study the Fe environments present in the different samples. Figure 4 displays Mössbauer spectra of sieved samples. All spectra were fitted with a dominant paramagnetic doublet component and a weaker central singlet. Those subspectra originate from the low symmetry paramagnetic Fe_{II} (96i) site and the highly symmetrical Fe_I (8b) site of the $La(Fe,Si)_{13}$ phase, respectively. In all cases, the quadrupolar splitting and the isomer shift of the doublet were found to be 0.47 (2) $mm{\cdot}s^{-1}$ and -0.04 (1) $mm{\cdot}s^{-1}$, respectively, and the isomer shift of the singlet was -0.09 (1) $mm{\cdot}s^{-1}$.

Their linewidths and the relative intensity between the two lines of the doublet were kept fixed to 0.35 mm·s^{-1} and 1, respectively. The absorption area ratio singlet/doublet (changing as 1:12-x [22,23,24]) was fixed to 0.093 according to a Si content x=1.2.

In addition, a set of three (for D_{100} and D_{25} samples) and five (for D_{300} sample) magnetic sextets (Table 1) were included in the fitting. These subspectra correspond to the different neighbourhood of Fe atoms in the bcc-Fe(Si) disordered phase. Their quadrupolar splitting, linewidth and the relative intensity between middle and inner lines were kept fixed during the fitting to 0 mm·s^{-1}, 0.35 mm·s^{-1} and 2, respectively, for all sextets. The Fe atomic fraction corresponding to the fcc-La(Fe,Si)$_{13}$ phase (singlet plus doublet sites) is shown in figure 2. Assuming the nominal composition, the Mössbauer results can be changed from at. % Fe to w. % (Figure 2). A very good agreement with XRD results is observed.

Figure 5 shows the specific magnetization as a function of temperature, $\sigma(T)$, for all samples at an applied magnetic field of 0.5 T. The ferro-paramagnetic transition temperature of the fcc-La(Fe,Si)$_{13}$ phase (~186 K, in agreement with values found in literature [8]) does not show significant changes with particle size. The magnetization has the contribution of the two phases at low temperature but, at high temperatures, only the bcc-Fe(Si) has a significant value. In order to estimate the magnetization phase fraction, X_σ, corresponding to the fcc-La(Fe,Si)$_{13}$ phase, the contribution of the bcc-Fe(Si) has been linearly extrapolated down to 150 K to be subtracted to the measured specific magnetization at this temperature and normalized to σ at 150 K. X_σ decreases from 62 % for D_{25} to 56 % for D_{100} and 2 % for D_{300}, in qualitative agreement with the observed variation of the fcc-La(Fe,Si)$_{13}$ phase fraction previously shown. In the case of the bulk sample X_σ = 12 % which corresponds to an intermediate value. Therefore, from magnetic measurements, we get an enhancement of five times in the amount of fcc phase after powder size selection. This value could be achieved just discarding the largest particles.

Figure 6 shows the temperature dependence of the magnetic entropy change for the studied samples. The curve of the bulk sample shows a maximum $|\Delta S_M|$ value of 3.1 J kg^{-1}K^{-1}, for an internal magnetic field change of 1 T. This value, lower than those reported in the literature for this type of compositions, is due to the high content of bcc-Fe(Si) phase. For sieved samples, as the particle size of the sample decreases the maximum value of $|\Delta S_M|$ at 1 T, increases from 0.7 J kg^{-1}K^{-1} for D_{300} to 6.2 J kg^{-1}K^{-1} and

7.8 J $kg^{-1}K^{-1}$ for D_{100} and D_{25} samples, respectively, in agreement with the increase of the fcc-La(Fe,Si)$_{13}$ phase fraction reported above. Assuming a linear dependence of the peak value of $|\Delta S_M|$ with the fcc phase fraction, a value of 11 J $kg^{-1}K^{-1}$ at 1 T for an ideal 100 % fcc-La(Fe,Si)$_{13}$ phase can be extrapolated.

Conclusions

Arc melted bulk material with nominal composition $LaFe_{11.8}Si_{1.2}$ was annealed for 7 days at 1373 K, grinded and sieved to obtain powder samples with different particle size ranges. Microstructure and Fe environment results show that the samples are formed by two majority phases, fcc-La(Fe,Si)$_{13}$ and bcc-Fe(Si), and a residual tetragonal LaFeSi. It was evidenced that the fraction of fcc-La(Fe,Si)$_{13}$ phase increases as the powder particle size decreases. The particle size after the grinding process is affected by the brittleness of the phases. A larger amount of the brittle La(Fe,Si)$_{13}$ intermetallic phase yields to easier comminuting of the powder particles.

The Curie temperature of La(Fe,Si)$_{13}$ phase does not show significant changes with the powder particle size and is in agreement with the calculated composition from the microstructural study. The peak value of the magnetic entropy change monotonously increases as the powder particle size decreases, in agreement with the increase of the fcc-La(Fe,Si)$_{13}$ phase fraction.

Size selection of powder particles is proposed as a successful and simple route to enhance the volume fraction of fcc-Fe(LaSi)$_{13}$ and, consequently, the magnetocaloric response of the material.

Acknowledgements

This work was supported by the Spanish MINECO and EU FEDER (project MAT2013-45165-P) and the PAI of the Regional Government of Andalucía. L.M. Moreno-Ramírez acknowledges a FPU fellowship from the Spanish MECD.

Figure captions

Figure 1. X-ray diffraction patterns and the corresponding Rietveld fitting for sieved samples. Diffraction lines corresponding to residual tetragonal LaFeSi phase are marked with asterisks.

Figure 2. Phase fraction of the fcc-La(Fe,Si)$_{13}$ obtained by X-ray diffraction (w. %) and Mössbauer spectrometry (at. % Fe and w.%) as a function of the minimum particle size of each studied range.

Figure 3. Scanning electron microscopy images in backscattered electrons mode for a) D_{300} sample (particle size in the range of D >300 μm) and b) D_{25} sample (25< D <100 μm).

Figure 4. Mössbauer spectra and their corresponding fitting for sieved samples.

Figure 5. Temperature dependence of the specific magnetization at 0.5 T for all studied samples. The dashed lines show the extrapolation of the magnetization of the bcc-Fe(Si) phase to low temperatures.

Figure 6. Temperature dependence of the magnetic entropy change at 1 T for all studied samples.

Figure 1

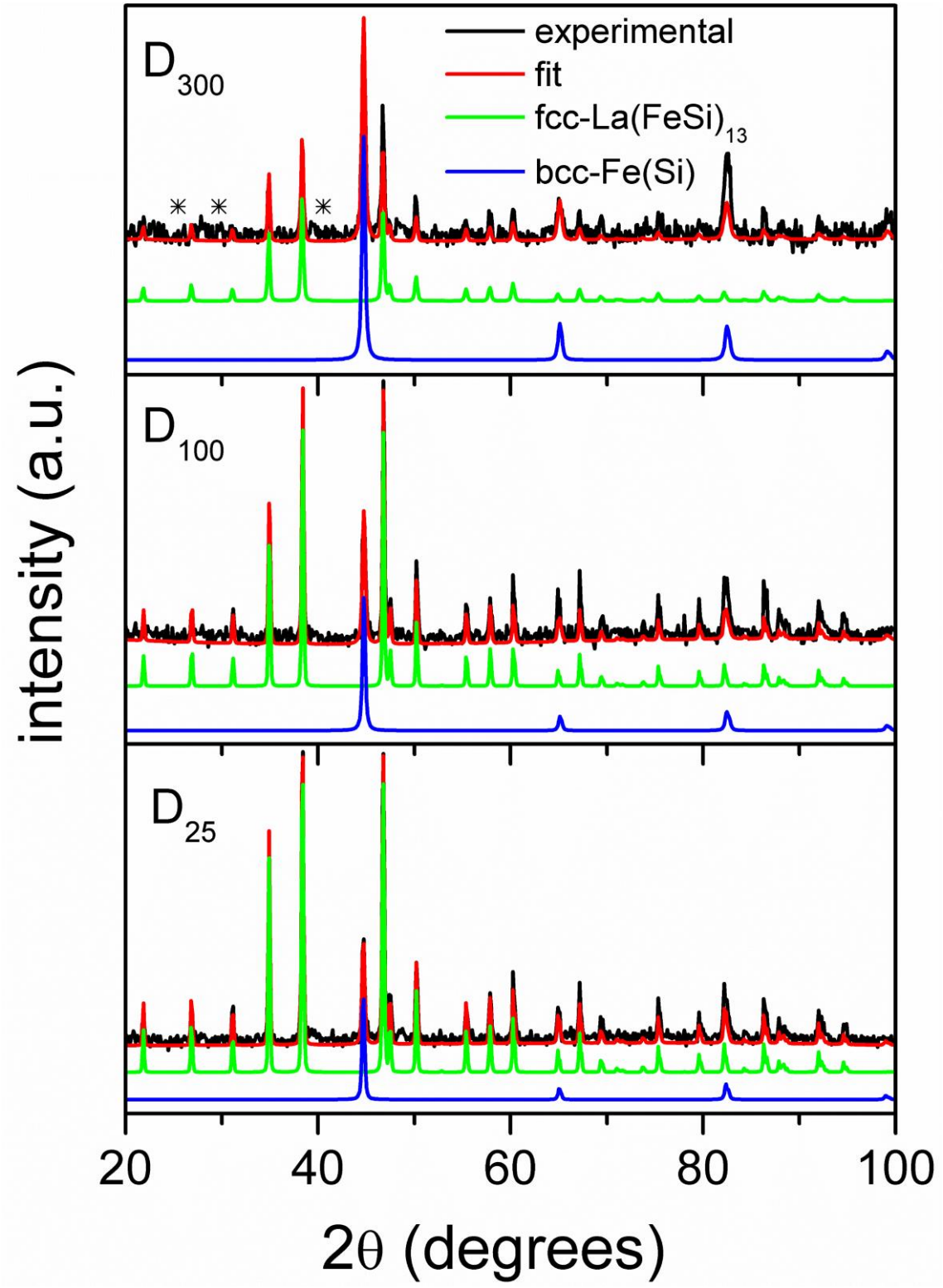
experimental
fit
fcc-La(FeSi)13
bcc-Fe(Si)
D300
D100
D25
intensity (a.u.)
20
40
60
80
100
2θ (degrees)

Figure 2

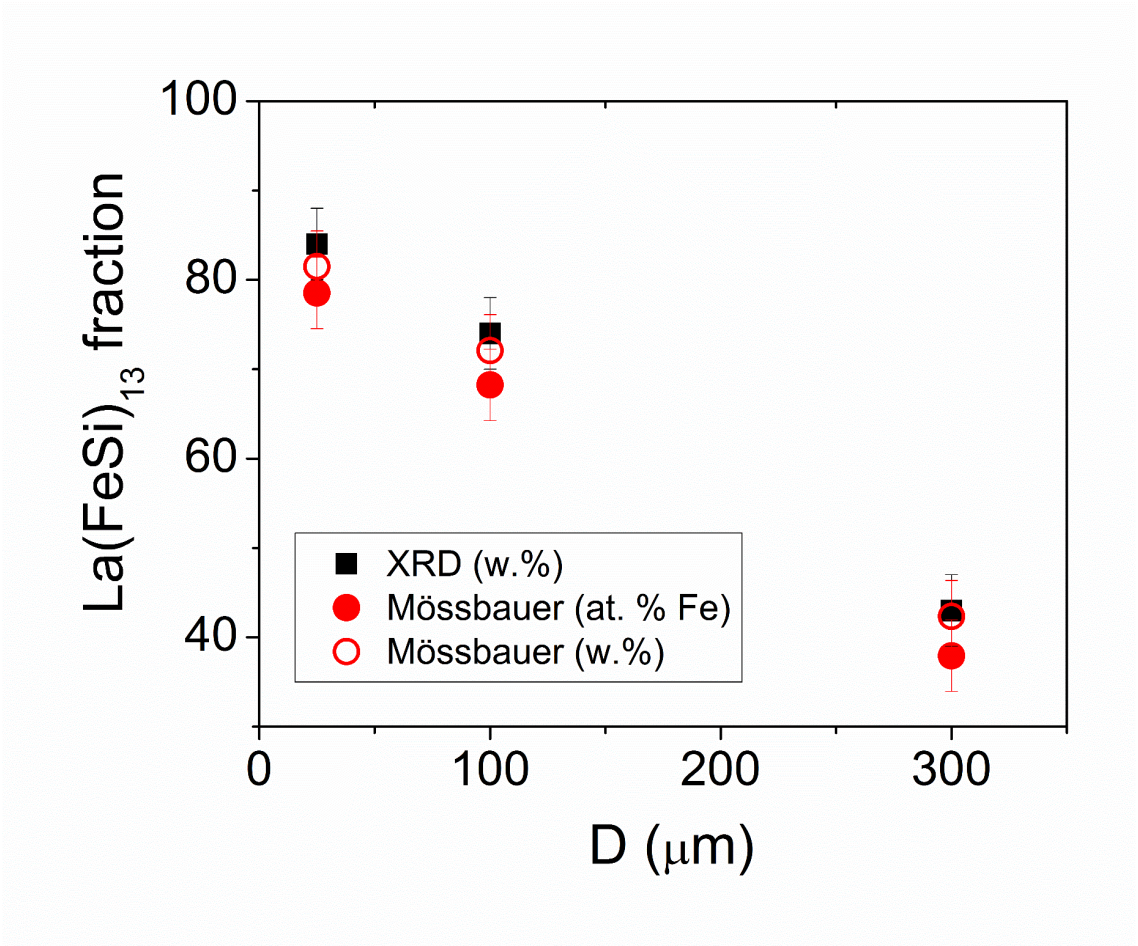
100
80
60
40
La(FeSi)13 fraction
0
100
200
300
D (μm)
XRD (w.%)
Mössbauer (at. % Fe)
Mössbauer (w.%)

Figure 3

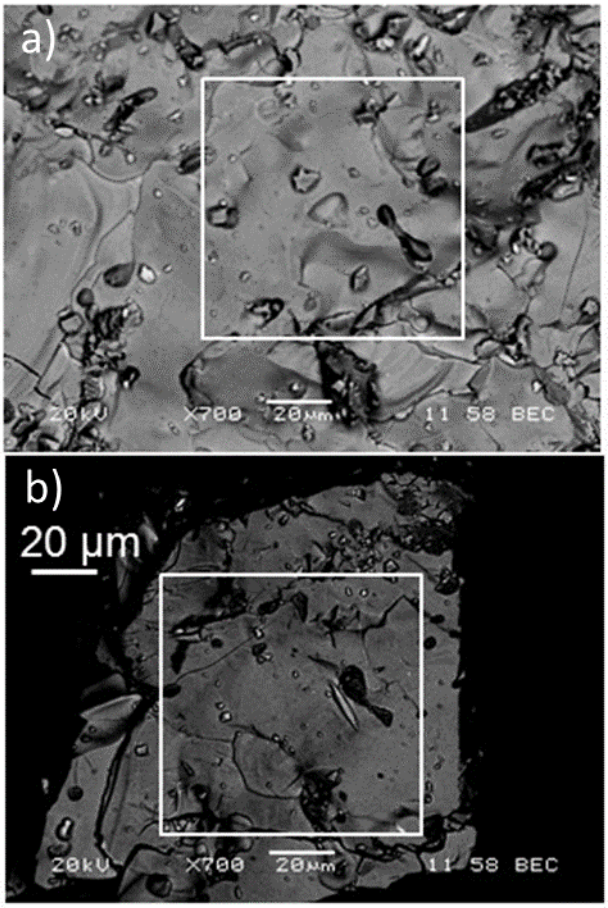

Figure 4

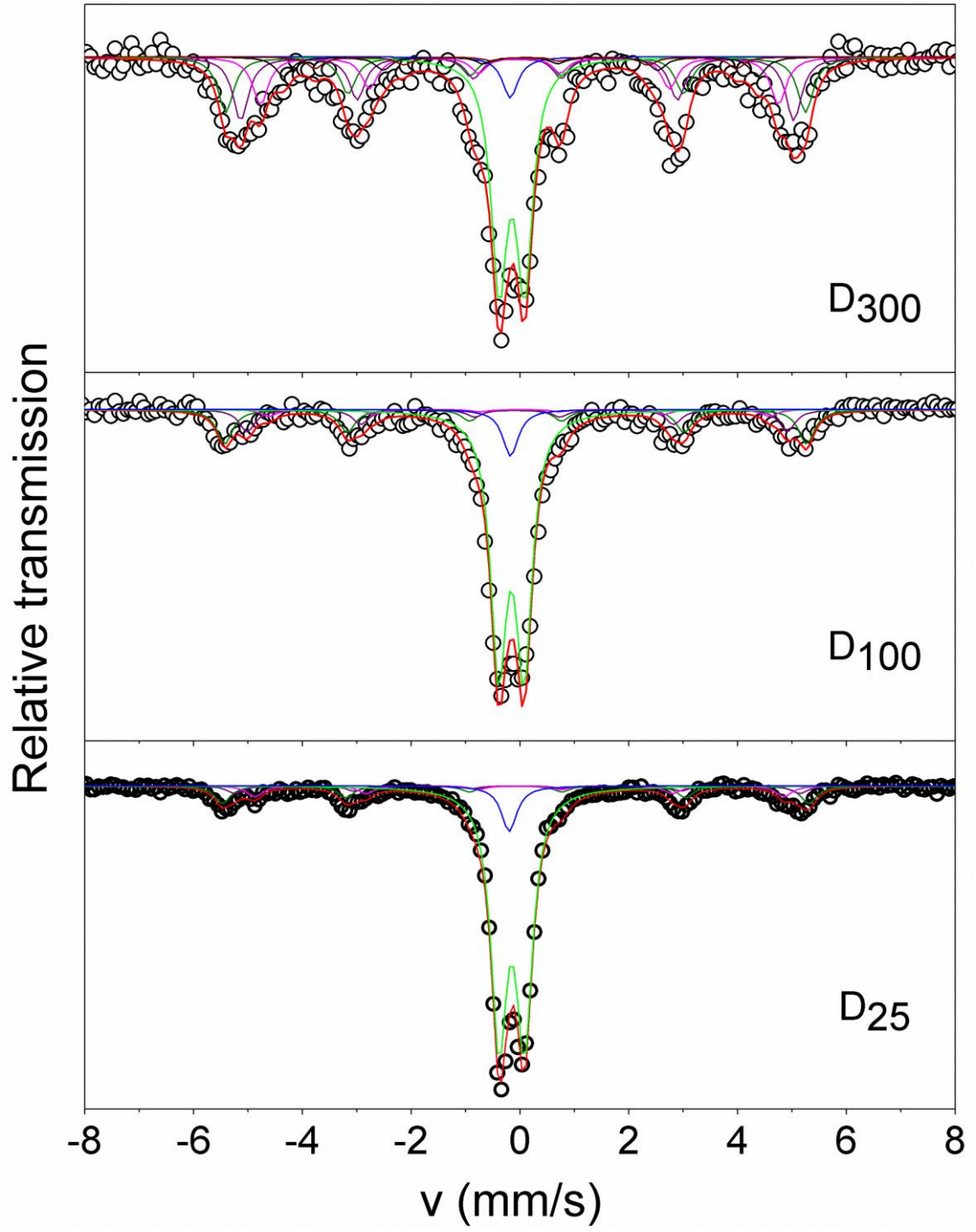

Figure 5

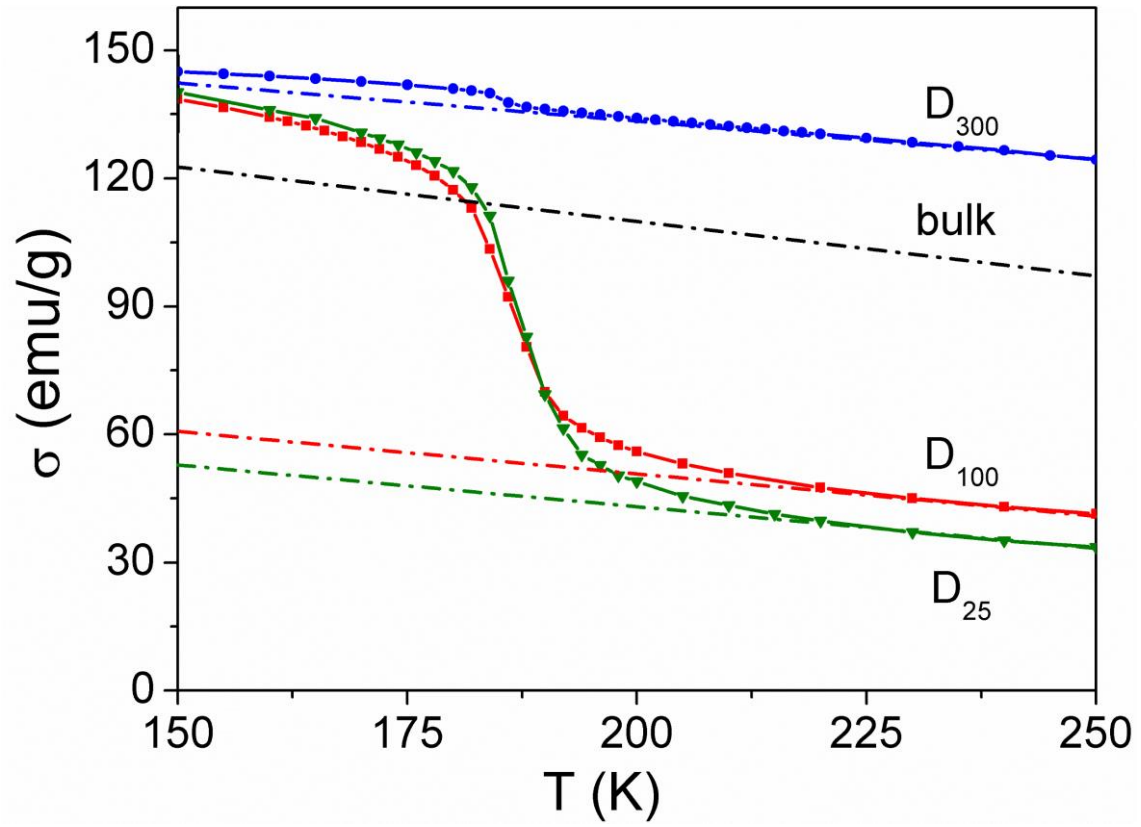

Figure 6

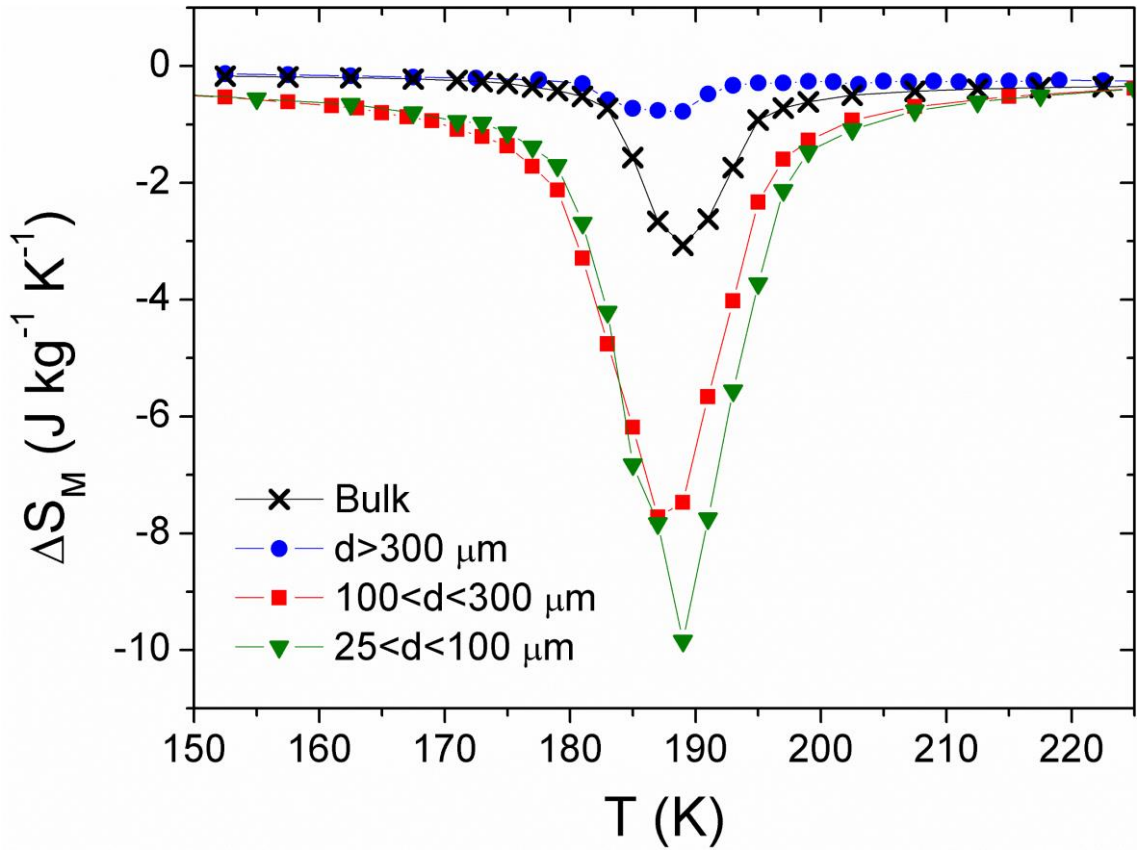

Table 1. Mössbauer parameters of the sextets corresponding to bcc-Fe(Si) phase, obtained from the fitting of the RT spectra.

	D_{300}					D_{100}			D_{25}		
bcc-Fe(Si) (sextet)	#1	#2	#3	#4	#5	#1	#2	#3	#1	#2	#3
B_{hf} ± 0.5 T	33.4	31.5	29.5	27.0	24.0	33.1	30.8	28.5	33.4	32.2	30.1
IS ± 0.01 mm/s	0.03	0.06	0.10	0.12	0.22	0.03	0.06	0.10	0.03	0.06	0.10
Area sextet ± 0.5 %	17.3	19.9	14.9	6.2	3.7	17.2	11.1	3.5	10.4	4.5	6.6
Area bcc ± 2 %	62					32			22		

References

[1] K. A. Gschneidner, Jr. and V. K. Pecharsky, Annu. Rev. Mater. Sci. 30 (2000) 387.

[2] E. Brück, O. Tegus, D. T. C. Thanh, and K. H. J. Buschow, J. Magn. Magn. Mater. 310 (2007) 2793.

[3] V. Franco, J. S. Blázquez, B. Ingale, and A. Conde, Annu. Rev. Mater. Res. 42 (2012) 305.

[4] K. A. Gschneidner, Jr., V. K. Pecharsky, Phys. Rev. Lett. 78 (1997) 4494.

[5] O. Tegus, E. Brück, K.H.J. Buschow, F.R. de Boer, Nature 415 (2002) 150.

[6] F.X. Hu, B.G. Shen, J.R. Sun, Z.H. Zheng, G.H. Rao, X.X. Zhang, App. Phys. Lett. 78 (2001) 3675.

[7] T. Krenke, E. Duman, M. Acet, E.F. Wassermann, X. Moya, L. Mañosa, A. Planes, Nat. Mater. 4 (2005) 450.

[8] K. A. Gschneidner, Jr., V. K. Pecharsky, A.O. Tsokol, Rep. Prog. Phys. 68 (2005) 1479

[9] K. Löwe, J.Liu, K. Skokov, J.D. Moore, H. Sepehri-Amin, K. Hono, M. Katter, O. Gutfleisch, Acta Mater. 60 (2012) 4268.

[10] B.R. Hansen, L.T. Kuhn, C.R.H. Balh, M. Lundberg, C. Anacona-Torres, M. Katter, J. Mag. Mag. Mater. 322 (2010) 3447.

[11] K. Fukamichi, A. Fujita, S. Fujieda, J. Alloys Comp. 408-412 (2006) 307.

[12] A. Fujita, Y. Akamatsu, K. Fukamichi, J. Appl. Phys. 85 (1999) 4756.

[13] B.G. Shen, J.R. Sun, F.X. Hu, H.W. Zhang, Z.H. Cheng, Adv. Mater. 21 (2009) 1.

[14] W.H. Tang, J.K. Liang, G.H. Rao, X. Yan, Phys. Stat. Sol. a 141 (1994) 217.

[15] F.X. Hu, L. Chen, J. Wang, L.F. Bao, J.R. Sun, B.G. Shen, Appl. Phys. Lett. 100 (2012) 072403.

[16] J. Liu, J.D. Moore, K.P. Skokov, M. Krautz, K. Löwe, A. Barcza, M. Katter and O. Gutfleisch, Scripta Mater. 67 (2012) 584.

[17] R.A. Brand, J. Lauer, D.M. Herlach, J. Phys. F: Met. Phys. 13 (1983) 675.

[18] J.M.D. Coey: Magnetism and Magnetic Materials, Cambridge University Press, New York, NY, 2010, p. 39.

[19] V. Franco, B.C. Dodrill, C. Radu, Magn. Bus. Technol., 13 (Winter 2014), p.8 The analysis software and accompanying Application Note is available at: http://www.lakeshore.com/products/Vibrating-Sample-Magnetometer/pages/MCE.aspx

[20] E. Gaffet, N. Malhouroux, M. Abdellaoui, J. Alloys Comp. 194 (1993) 339.

[21] K. Niitsu, S. Fijieda, A. Fujita, R. Kainuma, J. Alloys Comp. 578 (2013) 220.

[22] H.H. Hamdeh, H. Al-Ghanem, W.M. Hikal, S.M. Taher, J.C. Ho, D.T.K. Anh N.P. Thuy, N.H. Duc and P.D. Thang, J. Magn. Magn. Mater. 269 (2004) 404.

[23] F. Wang, G.J. Wang, F.X, Hu, A. Kurbakov, B.G. Shen, Z. H. Cheng, J. Phys.: Condens. Matter 15 (2003) 5269.

[24] S. I. Makarov, M. Krautz, S. Salamon, K. Skokov, C. S. Teixeira, O. Gutfleisch, H. Wende, W. Keune, J. Phys. D: Appl. Phys. 48 (2015) 305006.